

# Growth and Characterization of $\text{In}_x\text{Ga}_{1-x}\text{As}/\text{GaAs}_{1-y}\text{P}_y$ Strained-Layer Superlattices with High Values of $y$ ( $\sim 80\%$ )

J.P. SAMBERG,<sup>1,3</sup> C.Z. CARLIN,<sup>2</sup> G.K. BRADSHAW,<sup>2</sup> P.C. COLTER,<sup>2</sup>  
and S.M. BEDAIR<sup>2</sup>

1.—Department of Material Science and Engineering, North Carolina State University, Raleigh, NC 27695, USA. 2.—Department of Electrical and Computer Engineering, North Carolina State University, Raleigh, NC 27695, USA. 3.—e-mail: joshsamberg@gmail.com

Strained-layer superlattice (SLS) structures, such as InGaAs/GaAsP lattice matched to GaAs, have shown great potential in absorption devices such as photodetectors and triple-junction photovoltaic cells. However, until recently they have been somewhat hindered by their usage of low-phosphorus GaAsP barriers. High-P-composition GaAsP was developed as the barrier for InGaAs/GaAsP strained-layer superlattice (SLS) structures, and the merits of using such a high composition of phosphorus are discussed. It is believed that these barriers represent the highest phosphorus content to date in such a structure. By using high-composition GaAsP the carriers are collected via tunneling (for barriers  $\leq 30$  Å) as opposed to thermionic emission. Thus, by utilizing thin, high-content GaAsP barriers one can increase the percentage of the intrinsic in a *p-i-n* structure that is composed of InGaAs wells in addition to increasing the number of periods that can be grown for given depletion width. However, standard SLSs of this type inherently possess undesirable compressive strain and quantum size effects (QSEs) that cause the optical absorption of the thin InGaAs SLS wells to shift to higher energies relative to that of bulk InGaAs of the same composition. To circumvent these deleterious QSEs, stress-balanced, pseudomorphic InGaAs/GaAsP staggered SLSs were grown. Staggering was achieved by removing a portion of one well and adding it to an adjacent well. The spectral response obtained from device characterization indicated that staggering resulted in thicker InGaAs films with reduced cutoff energy. Additionally, these data confirm that tunneling is a very effective means for carrier transport in the SLS.

**Key words:** Superlattice, strain-balanced, tunneling, InGaAs, GaAsP, photovoltaic

## INTRODUCTION

III–V semiconductors are useful in optoelectronic applications; however, not all desired band gaps are available in alloys lattice matched to available substrates. This limitation can be overcome by using metamorphic and pseudomorphic structures. Metamorphic structures have issues with defects which can be alleviated but not eliminated.

Individually, pseudomorphic layers are limited by the critical layer thickness, after which relaxation occurs. This deleterious relaxation limits the total thickness of an individual pseudomorphic layer to the range of a few nanometers to a few tens of nanometers. To avoid relaxation, many pseudomorphic layers can be grown by balancing compressive and tensile layers in a structure termed a strain-balanced, strained-layer superlattice (SLS) structure. The concept of the strain-balanced InGaAs/GaAsP superlattice, lattice-matched to GaAs,

(Received August 17, 2012; accepted November 28, 2012;  
published online December 20, 2012)

was developed in the 1980s and used in several structures such as light-emitting diodes (LEDs),<sup>1</sup> solar cells,<sup>2</sup> and buffer layers to reduce defects<sup>3</sup> in heterostructures.

One application where strain-balanced SLSs are particularly promising is in the InGaP/GaAs/Ge triple-junction (3J) photovoltaic cell, wherein increased efficiency can be obtained by extending the absorption of the middle GaAs or top InGaP cell to longer wavelengths and improving the spectral matching between the three subcells. The first lattice-matched strain-balanced superlattice solar cells were fabricated for solar spectrum matching in tandem cells.<sup>2</sup> After efficient InGaP/GaAs tandems were developed, quantum wells (QWs) within the intrinsic region of a  $p-i-n$  solar cell were suggested as a means to improve spectral matching.<sup>4</sup> An SLS system consisting of InGaAs/GaAsP has potential to improve spectral matching of 3J photovoltaics (PVs).

The design of the SLS depends on several parameters: mainly the strain balance of the SLS, the critical layer thickness of both the individual pseudomorphic layers and the SLS as a whole, and the requirement for efficient carrier transport across the barriers in both the conduction and valence bands. In this paper we describe the growth and characterization of an SLS using very high  $\text{GaAs}_{1-y}\text{P}_y$  phosphorus compositions to create a high band gap barrier layer. The advantages of using high content phosphorus barriers are as follows: first, high GaP composition will allow for thicker  $\text{In}_x\text{Ga}_{1-x}\text{As}$  optical absorbing wells while maintaining strain-balance conditions. Second, high GaP content will allow for thin barriers, resulting in an  $i$ -layer comprising mainly the InGaAs absorption layers. This will enhance the gain in  $J_{\text{SC}}$  as compared with that of a GaAs cell. Third, a thin barrier (with high GaP composition) will allow carriers to be transported by tunneling, as demonstrated in Fig. 1. It can be shown, for example, that for a SLS consisting of  $\text{In}_{0.15}\text{Ga}_{0.85}\text{As}/\text{GaAs}_{0.2}\text{P}_{0.8}$ ,  $>75\%$  of the  $i$ -layer is composed of absorbing InGaAs wells while maintaining carrier transport efficiency close

to 100% via tunneling. This tunneling approach is advantageous with respect to other approaches that utilize thermionic emission for carrier transport.<sup>5</sup> The latter approach requires thick ( $>200$  Å), low (6% P) GaAsP content barriers which results in only  $\sim 25\%$  of the  $i$ -layer being the InGaAs absorbing wells.

The use of thin, high-content GaP barriers results in InGaAs wells which are also relatively thin (50 Å to 100 Å), and the problem is compounded as one moves to higher indium compositions of InGaAs while maintaining strain-balance conditions. Thus, due to these fairly thin wells, there will be an undesirable shift in the threshold energy of the absorbed photons due to quantum size effects (QSEs).

To reduce the impact of the QSEs, we have devised the concept of a staggered SLS.<sup>6</sup> In this system, the thickness of one well is increased at the expense of an adjacent well. The period of the staggered SLS is thus doubled for all values of  $x$  and includes two wells and two barriers. However, the average-zero stress-balance condition remains constant. Thus, the stress in the structure was balanced for every period of two QWs. A schematic of the staggered SLS is presented in Fig. 2. This staggered SLS with two GaAsP barriers per period can only be implemented in a structure that utilizes thin GaAsP layers containing high-composition GaP. While this staggering is expected to result in an extension of the band edge to longer wavelength, it is imperative that the InGaAs wells do not exceed their critical layer thickness (CLT).

This paper describes methods to achieve  $\text{GaAs}_{1-y}\text{P}_y$  with high phosphorus composition barriers in SLS while maintaining strain-balanced conditions, and presents a staggered SLS structure which can be used to minimize and avoid QSEs. This paper presents the growth conditions for  $\text{GaAs}_{1-y}\text{P}_y$  with  $0.6 < y < 0.8$  as well as the growth of both the standard and staggered InGaAs/GaAsP SLS. Both materials and device aspects of these SLSs are discussed.

## EXPERIMENTAL PROCEDURES

All growth was carried out using a metalorganic chemical vapor deposition (MOCVD) growth system utilizing a homemade reactor that allows for fast

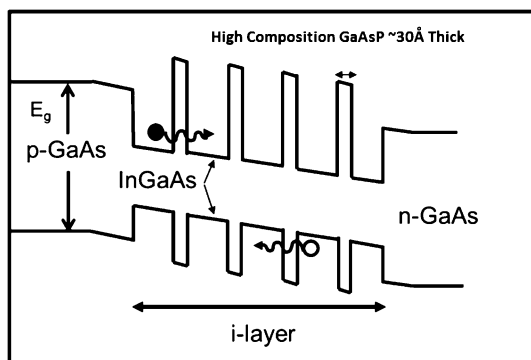


Fig. 1. General structure of the SLS, demonstrating tunneling through thin (30 Å), high-composition GaAsP barriers (GaP%  $>70\%$ ).

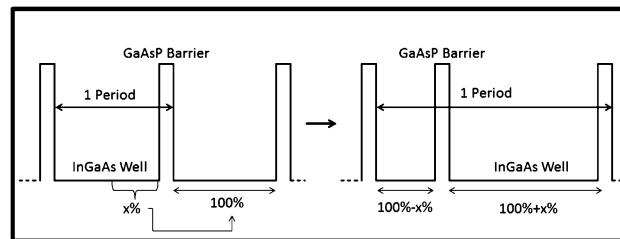


Fig. 2. Staggering of a standard SLS is achieved by moving a portion of one well to an adjacent well. A value of  $x = 50$  would result in a staggering ratio (thick well:thin well) of 3:1.

gas switching that is required for the growth of the  $\text{In}_x\text{Ga}_{1-x}\text{As}/\text{GaAs}_{1-y}\text{P}_y$  SLS. The structures are grown on (100) GaAs substrates oriented  $2^\circ$  to the (110) using tert-butylarsine (TBAs), tert-butylphosphine (TBP), trimethylindium (TMIn), and trimethylgallium (TMGa). The SLS structure is grown in the temperature range of  $570^\circ\text{C}$  to  $600^\circ\text{C}$  with a growth rate between  $6 \text{ \AA/s}$  and  $8 \text{ \AA/s}$ . This growth temperature range is a compromise between the high growth temperature preferred for GaAsP growth and the relatively lower growth temperature preferred for InGaAs. The InGaAs well compositions range from 5% to 20% indium, while the GaAsP barrier compositions range from 70% to 85% phosphorus for SLSs. All samples were characterized initially with optical Nomarski microscopy followed by x-ray diffraction (XRD). Optical microscopy was performed with an Olympus BX41 microscope fitted with a Nikon D3000 camera through the use of an Alexis Scientific adaptor. Optical microscopy is a very useful and easy characterization tool to determine if the SLS structure has relaxed, as crosshatching can be seen for unbalanced superlattices. The superlattice was characterized with the use of a Philips PANalytical X'Pert to determine the superlattice period, layer thicknesses, and balance conditions. The nominal thickness of the GaAsP barriers for strain-balanced superlattices was  $\sim 30 \text{ \AA}$  for all samples that were shown to have tunneling probabilities of about 100%.<sup>7</sup> InGaAs well thickness was determined via the zero-stress balance method for varying indium compositions. To evaluate the effect of staggering, samples with alternating thicknesses of InGaAs layers, as shown in Fig. 2, were grown with adjacent well thickness ratios of 1:1, 3:1, and 5.667:1. The conventional SLS device consisted of 20 to 40 periods of alternating layers, while the staggered SLS, by the definition of its period, consisted of 10 to 20 periods. As a control, a standard GaAs cell lacking a superlattice or intrinsic layer was grown.

Devices were fabricated by conventional contact photolithography as  $2.5 \text{ mm} \times 2.5 \text{ mm}$  etched mesas with electron beam evaporated metallization consisting of Ni/AuGe/Au  $n$ -type ohmic contacts and Ti/Pd/Ag  $p$ -type ohmic contacts. The metallization was annealed at  $400^\circ\text{C}$  for 40 s. The cells were fabricated without an antireflective (AR) coating. The fabricated devices were characterized with an Oriel 1-kW solar simulator at 1 sun illumination (AM 1.5 filter) in order to determine the open-circuit voltage ( $V_{\text{OC}}$ ), the short-circuit current ( $I_{\text{SC}}$ ), and the fill factor. A Newport Cornerstone 260  $\frac{1}{4}$  m monochromator coupled with a tungsten halogen light source provided the illumination for spectral response measurements.

## RESULTS AND DISCUSSION

The phosphorus composition as it relates to the TBP flow is shown in Fig. 3. All TBAs and TMGa

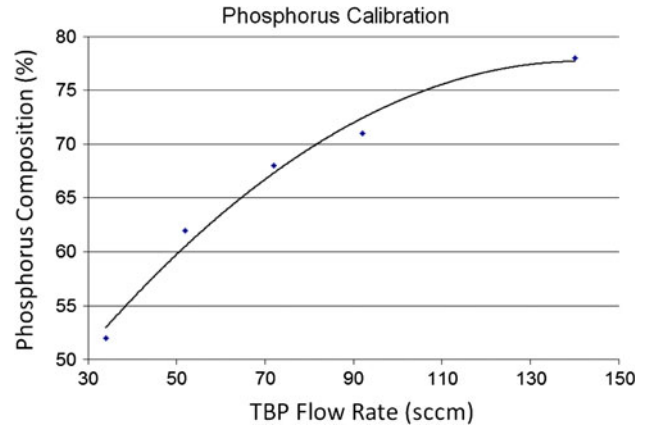


Fig. 3. Phosphorus calibration with TBAs flow rate of 20 sccm, TMGa flow rate of 2 sccm, and substrate temperature of  $600^\circ\text{C}$ .

flow rates for these calibrations were 20 sccm and 2 sccm, respectively, with bubbler temperatures of  $5.2^\circ\text{C}$  and  $0.0^\circ\text{C}$ , respectively. A substrate temperature of  $600^\circ\text{C}$  was used for the growth. As can be seen, the phosphorus composition reaches a saturation point for a given substrate temperature. It is near this saturation that we observed the most reproducible growth with respect to the SLS; the reasons for this phenomenon may be explained in multiple ways. When saturated, any variations with respect to TBP bubbler temperature, TBP bubbler pressure, and system pressure will be minimized within the growth itself. Additionally, we were able to obtain phosphorus compositions of 85% and higher by changing the substrate temperature. However, it was observed that higher substrate temperature was accompanied by greater difficulty in obtaining good-quality SLSs. It is posited that, due to the higher temperature, desorption of the arsenic species becomes too high for the indium wells, which results in indium and gallium droplets on the sample, ruining the morphology. These SLSs consist of  $\text{InGaAs}/\text{GaAs}_{0.25}\text{P}_{0.75}$ , and we believe this to be the highest phosphorus composition reported and used in strained-layer superlattice (SLS) structures. Optical microscopy can be used as a quick indication for the onset of relaxation in the SLS, as the relaxation manifests itself as a characteristic crosshatching of the sample surface.

To balance the SLS, a zero-stress balance method was utilized:<sup>8</sup>

$$\alpha_{\text{sub}} = \frac{A_{\text{In}}t_{\text{In}}a_{\text{In}}a_{\text{P}}^2 + A_{\text{Pt}}t_{\text{P}}a_{\text{P}}a_{\text{In}}^2}{A_{\text{In}}t_{\text{In}}a_{\text{P}}^2 + A_{\text{Pt}}t_{\text{P}}a_{\text{In}}^2},$$

where  $\alpha_{\text{sub}}$ ,  $a_{\text{In}}$ ,  $a_{\text{P}}$  are the lattice constants of the substrate, InGaAs wells, and GaAsP barriers, respectively,  $t_{\text{In}}$  and  $t_{\text{P}}$  are the well and barrier thicknesses, and  $A_{\text{In}}$ ,  $A_{\text{P}}$  is a stiffness parameter for the InGaAs wells and GaAsP barriers, respectively.

The stiffness parameters were calculated using the elastic stiffness coefficients for each material:

$$A = C_{11} + C_{12} - \frac{2C_{12}^2}{C_{11}}$$

When dealing with ternary compounds it is assumed that the elastic coefficients,  $C_{11}$  and  $C_{12}$ , can be linearly interpolated from the two binary materials composing the ternary compound. However, while this is fairly accurate near the peripheries ( $\pm 20\%$  of the endpoints) of the ternary compound composition, it becomes problematic the farther one shifts from the peripheries, as many ternary compounds have unknown bowing parameters that must be considered. Additionally, the zero-stress balance equation is based solely on a strain energy analysis, not taking into account any kinetic barriers.<sup>8</sup> Nevertheless, balanced SLS have been successfully grown using this method. Figure 4 reports the values obtained using this model with different InGaAs well composition thicknesses with respect to  $\text{GaAs}_{0.2}\text{P}_{0.8}$  barrier thicknesses. The horizontal bold line represents the barrier thickness limit for tunneling of the minority carriers. Figure 4 is used as a guide line for the strain adjustments for the different SLS compositions studied in this work.

In addition to helping determine the quality of the SLS, XRD was also used to determine the thickness of the periods in the SLS and to verify that zero-stress conditions were met. The periodic satellite fringes were used to determine the thickness of a period in the SLS by:

$$\sin(\theta_{n\pm 1}) - \sin(\theta_n) = \frac{n\lambda}{2t},$$

where  $\theta_{n\pm 1}$  or  $n$  is the Bragg angle for the  $n \pm 1$  or  $n$  satellite fringe,  $\lambda$  is the source wavelength, and  $t$  is the thickness of each period comprising the In wells, phosphorus barriers, and GaAs transition layers.

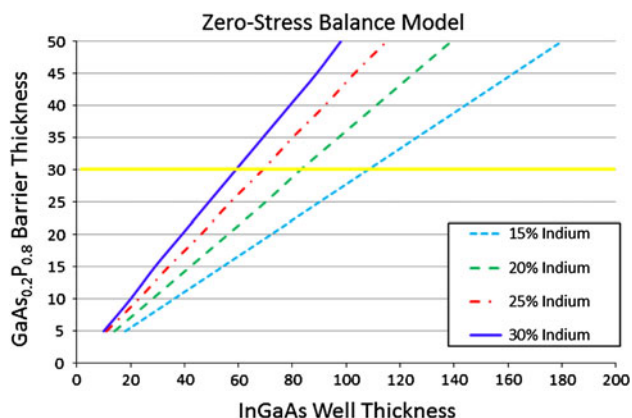


Fig. 4. Zero-stress balance for  $\text{GaAs}_{0.2}\text{P}_{0.8}$  barriers. The horizontal line represents the optimum barrier thickness that balances minority carrier transport and QSEs.

The XRD analysis for three samples is presented in Fig. 5. Figure 5a shows the XRD data collected from a normal SLS consisting of  $\text{In}_{0.15}\text{Ga}_{0.85}\text{As}/\text{GaAs}_{0.2}\text{P}_{0.8}$ . The peaks are well defined with relatively narrow full-width at half-maximum (FWHM) values. There appears to be some broadening of the peaks on the indium side ( $< 66.04^\circ$ ) of the substrate peak. This could be due to a partial relaxation of the sample. Optically, no crosshatching was observed for this normal SLS. Periodicity calculations for this sample yield periods of  $\sim 150$  Å. This indicates that the wells for this normal SLS are around 115 Å and are balanced by 27 Å wells, with the remainder comprising two GaAs layers that are deposited in the interfaces of the wells and barriers. These values agree very well with the zero-stress calculations, indicating great control over the growth of the SLS. Figure 5b is for a moderately staggered (1.5:1) SLS. The FWHM values of these peaks are the narrowest of the three displayed, and optically the surface was very clean with no crosshatching, indicating that the structure was completely strained. Periodicity calculations for this structure yield a period thickness of  $\sim 300$  Å. This is twice that found for Fig. 5a, which is to be expected as any staggering ratio effectively doubles the period. This periodicity gives well thicknesses of 138 Å and 92 Å and a barrier thickness of 27 Å with the remainder being GaAs transition layers. Figure 5c shows XRD data for a heavily staggered (5.667:1) SLS. Optically this sample displayed some crosshatching, and this is reflected in the FWHM values of the satellite peaks. The crosshatching was not systemic, however. This nonsystemic crosshatching indicates that it may be possible to stagger SLS structures to a ratio of 5.667:1 while maintaining pseudomorphic growth conditions. Periodicity calculations give a period thickness of 280 Å with well thicknesses of 176 Å and 31 Å and barrier thickness of 25 Å. The change of period thickness is also indicative of relaxation.

Device  $p$ - $i$ - $n$  structures were grown utilizing both conventional and staggered SLSs as the  $i$ -layer to evaluate their effect on device parameters. Staggering ratios of 3:1 ( $x = 50$ ) and 5.667:1 ( $x = 70$ ) were utilized for this analysis. It was determined from the spectral response (Fig. 6) that improved extension was obtained with the higher staggering ratios. Both XRD and optical microscopy showed that the staggered SLS structures are strained with no relaxation occurring. Additionally, the fairly high external quantum efficiency (EQE) (without AR coating) seen in Fig. 6 indicates that carrier transport by means of tunneling occurs with close to 100% efficiency.  $I$ - $V$  measurements were also performed. Fill factors of 81.2% and 79.9% were obtained from these  $I$ - $V$  measurements for both the staggering ratio of 3:1 and 5.667:1, respectively. Additionally,  $V_{\text{OC}}$  values of 0.97 V and 0.95 V were obtained for the staggering ratios of 3:1 and 5.667:1, respectively. Comparing these results with those

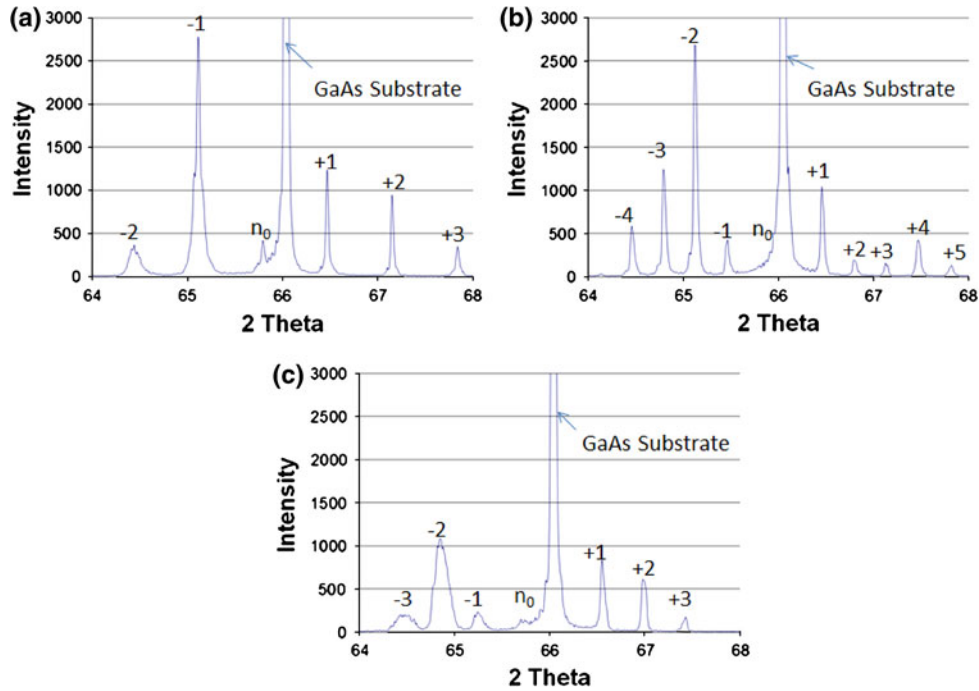


Fig. 5. (004) XRD data for In<sub>0.15</sub>Ga<sub>0.85</sub>As/GaAs<sub>0.2</sub>P<sub>0.8</sub> normal SLS (a), 1.5:1 staggered SLS (b), and 5.667:1 staggered SLS (c).

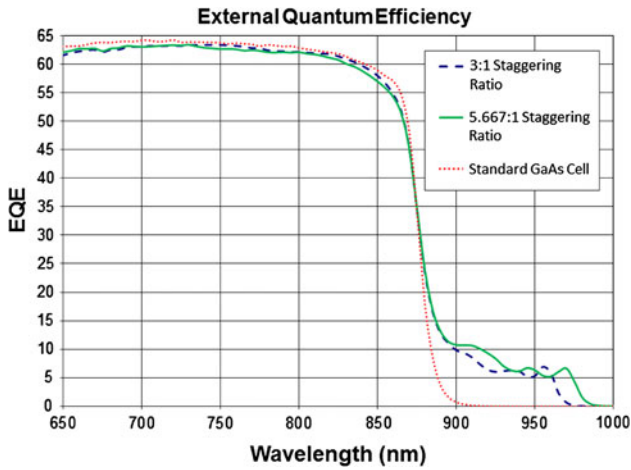


Fig. 6. External quantum efficiency for a standard GaAs cell and two staggered *p-i-n* cells with staggering ratios of 3:1 and 5.667:1. Extension of the band edge is observed when the SLS staggering is increased.

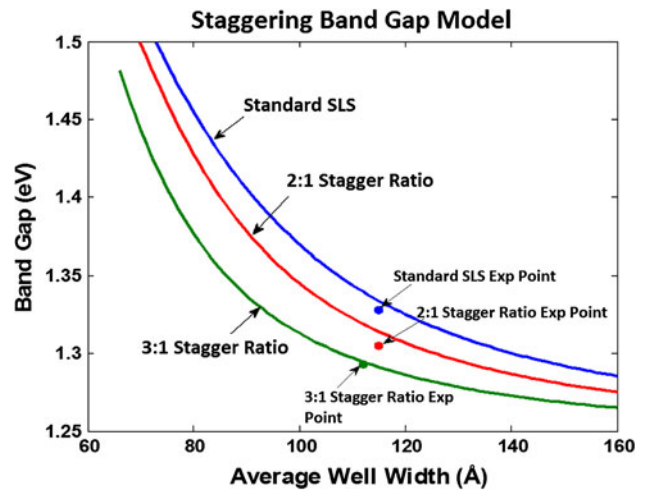


Fig. 7. Staggered band gap model showing how staggering affects the band edge of the SLS.

obtained from the standard GaAs cell (fill factor of 81.4%,  $V_{OC}$  of 0.97 V), it is indicated that these staggered SLSs could offer an increase of about 0.7 mA/cm<sup>2</sup> in current with a minor reduction of fill factor and  $V_{OC}$ .

To investigate how staggering overcame QSEs, a model was developed and is presented in Fig. 7. From this model we determined that QSEs were reduced as the staggering ratio of 1:1 for our normal SLS was increased to 3:1. It should be noted that the *x*-axis value of average well width is the average of both the thick and thin InGaAs wells. This is used to

provide a normalized value, making it easier to compare a normal SLS and any permutations of staggering thereof. The model was compared with experimental results to see how well it matched up to the observed extension past the GaAs band edge. These results have been labeled on Fig. 7 and agree very well with the model.

### CONCLUSIONS

High-phosphorus-composition GaAsP (>75% P) was successfully grown by utilizing a saturation point

on a calibration curve. This high composition of GaAsP was grown in conjunction with InGaAs in a strained-layer superlattice structure where tunneling was the transport mechanism used to collect the minority carriers. Tunneling was only made possible by utilizing very thin barriers ( $\sim 30$  Å). While using thin, high-composition GaAsP barriers is advantageous when it comes to carrier transport and increasing the usable percentage of the SLS (the InGaAs wells make up a larger percentage of the SLS for structures utilizing tunneling as opposed to thermionic emission for carrier transport), they do impart some deleterious QSEs to the InGaAs wells. It was shown that these QSEs could be overcome by using a staggered SLS. We have shown that staggered SLSs result in further extension of the absorption edge when compared with the conventional SLS by minimizing the QSEs. Also, the staggered SLS shows very good EQE, indicating that tunneling is an efficient carrier transport. These advantages occur with little reduction in either  $V_{\text{OC}}$  or fill factor.

## ACKNOWLEDGEMENTS

The authors would like to thank the National Science Foundation (NSF) for their financial support of this work.

## REFERENCES

1. T. Katsuyama, Y.J. Yang, and S.M. Bedair, *IEEE Electron Device Lett.* 8, 240 (1987).
2. T. Katsuyama, M. Tischler, N.A. El-Masry, and S.M. Bedair, *Sol. Cells* 21, 413 (1987).
3. M.A. Tischler, T. Katsuyama, N. El-Masry, and S.M. Bedair, *Appl. Phys. Lett.* 46, 383 (1985).
4. A. Freundlich and I. Serdiukova, *Proceedings of the Second World Conference on Photovoltaic Solar Energy Conversion, Vienna, Austria* (1998), p. 3707.
5. N.J. Ekins-Daukes, J. Adams, I.M. Ballard, K.W.J. Barnham, B. Browne, J.P. Connolly, T. Tibbits, G. Hill, and J.S. Roberts, *Proc. SPIE* 7211, 72110L (2009).
6. P.C. Colter, C.Z. Carlin, J.P. Samberg, G.K. Bradshaw, and S.M. Bedair, *Phys. Status Sol. (a)* 208, 2884 (2011).
7. G.K. Bradshaw, C.Z. Carlin, P.C. Colter, J.L. Harmon, J.P. Samberg, and S.M. Bedair, *MRS Proceedings* (2009).
8. N.J. Ekins-Daukes, K. Kawaguchi, and J. Zhang, *Cryst. Growth Des.* 2, 287 (2002).